EPRIM: An approach of identifying cancer immune-related epigenetic regulators

Aiai Shi,[1,2,3] Chaohuan Lin,[4,5] Jilu Wang,[5,6] Ying'ao Chen,[4,5] Jinjin Zhong,[7] and Jie Lyu[1,2,8]

[1]Joint Centre of Translational Medicine, The First Affiliated Hospital of Wenzhou Medical University, Wenzhou 325035, People's Republic of China; [2]Joint Centre of Translational Medicine, Wenzhou Institute, University of Chinese Academy of Sciences, Wenzhou, Zhejiang 325001, People's Republic of China; [3]Institute of Theoretical Physics, Chinese Academy of Sciences, Beijing 100190, People's Republic of China; [4]Postgraduate Training Base Alliance of Wenzhou Medical University, Wenzhou, Zhejiang 325000, China; [5]Wenzhou Institute, University of Chinese Academy of Sciences, Wenzhou, Zhejiang 325000, People's Republic of China; [6]University of Chinese Academy of Sciences, Beijing 100049, People's Republic of China; [7]Wenzhou Key Laboratory of Biophysics, Wenzhou Institute, University of Chinese Academy of Sciences, Wenzhou, Zhejiang 325001, China; [8]Oujiang Laboratory (Zhejiang Lab for Regenerative Medicine, Vision and Brain Health), Wenzhou, Zhejiang 325001, People's Republic of China

Epigenetic regulation contributes to the dysregulation of gene expression involved in cancer biology. Nevertheless, the roles of epigenetic regulators (ERs) in tumor immunity and immune response remain basically unclear. Here, we developed the epigenetic regulator in immunology (EPRIM) approach to identify immune-related ERs and comprehensively dissected the ER regulation in tumor immune response across 33 cancers. The identified immune-related ERs were related to immune infiltration and could stratify cancer patients into two risk groups in multiple independent datasets. These patient groups were characterized by distinct immune functions, immune infiltrates, driver gene mutations, and prognoses. Furthermore, we constructed an immune ER-based signature and highlighted its potential utility in predicting clinical benefit from immunotherapy and selecting therapeutic agents. Taken together, our identification and evaluation of immune-related ERs highlight the usefulness of EPRIM for the understanding of ERs in immune regulation and the clinical relevance in evaluation of cancer patient prognosis and response to immune checkpoint blockade therapy.

INTRODUCTION

Tumors are complex ecosystems reflected by complicated and dynamic crosstalk among cellular and molecular components. The immune system is important for killing tumor cells and its dysregulation serves profound roles in cancer development.[1] Benefiting from cancer immunotherapy, the success of clinical treatment has been achieved in multiple cancers, including melanoma, and lung and gastric cancer.[2,3] However, tumor cells can evade immune surveillance by regulating immune-related pathways, such as loss of antigen presentation,[4,5] leading to limited clinical efficacy. Thus, understanding molecular mechanisms behind the dysregulated immune microenvironment is of great importance.

Epigenetics studies how environment factors cause the heritable events in a cellular phenotype, in contrast to the changes encoded in DNA sequences.[6] The heritable events usually confer covalent modifications to histones or nucleic acids (e.g., DNA methylation and histone acetylation), as key regulatory mechanisms behind cancer biology.[7,8] Recently, researchers have highlighted the role of epigenetic machinery in tumor immunity.[9] Epigenetic regulators (ERs), which made covalent modifications to confer those heritable epigenetic alternations (e.g., methyltransferases), emerged as crucial regulators in gene expression, affecting cell development and cancer progression.[10-13] Gene silencing against molecules linked to cancer provided an effective treatment strategy, and gene expression analysis was widely used for identifying such key molecules.[14,15] Recent progress in cancer studies demonstrated that ERs could modulate the tumor immune microenvironment.[8,16] For example, the expression of ER additional sex combs-like 2 (ASXL2) was correlated to immune infiltration and clinical outcomes for cancer patients.[17] The ER cat eye syndrome chromosome region candidate 2 (CECR2) expression promoted the proliferation or polarization of tumor-associated macrophages to drive tumor metastasis, and was nominated as a promising target through its depletion or inhibition for cancer treatment.[18] Lysine demethylase 3A (KDM3A) could suppress anti-tumor immunity by remodeling the T cell inflamed state and regulated immunotherapy response, and its depletion could sensitize tumors to immunotherapy in combination with other drugs.[19] Another study constructed an ER signature related to immune infiltration and immunotherapy response in liver cancer based on gene expression analysis.[20] Nevertheless, a detailed compilation and characterization of the ERs implicated in immune regulation and cancer treatment is still lacking.

Here, we developed the epigenetic regulator in immunology (EPRIM) method to identify immune-related ERs and characterized the identified ERs across 33 cancer types based on the integrated gene expression and immune profile data. Immune infiltrates and independent datasets analysis validated their potential roles in immune regulation. Furthermore, an immune ER-based signature that we constructed revealed its predictive potential for cancer patient survival and therapy response.

RESULTS

Pan-cancer identification of immune-related epigenetic regulator genes

Transcriptional profiles have been widely used to study the function of biological regulators in cancer. Our hypothesis is that ERs may be involved in immune regulation, if the ranked gene set of correlated genes of ERs can be enriched in specific gene sets in immune pathways. Based on this, we designed an approach termed EPRIM (epigenetic regulator in immunology) to infer ERs that have potential implications in immune regulation (Figure 1A). In brief, the gene expression data of tumor samples and the collected immune signature gene set were needed as the inputs. The effect of ER expression on immune pathways regulation was evaluated by their correlated signature genes after correcting for tumor purity. Gene set enrichment analysis (GSEA),[21] an intuitive method to measure the coherence of coordinately changed signature genes in the rank list, was used to prioritize ERs implicated in immune pathways. A correlation score combining the p value and enrichment score was defined to indicate the correlation of each significant ER-immune pathway pair.

To systematically identify the potential ERs contributing to immune pathway activity, we applied EPRIM to expression profiles of >10,000 cases across 33 cancer types from The Cancer Genome Atlas (TCGA) (Table S1). A comprehensive list of 690 ERs with their functional annotations (e.g., histone reader) was collected from our manual curation[22] (Table S2). In addition, we derived 17 gene sets indicating distinct immune pathways from the ImmPort database[23] (Table S3). EPRIM identified 585 from 690 ERs (84.8%) as immune pathway regulators. On average, ~85 ERs were significantly correlated with immune pathways (ranging from 22 in kidney chromophobe [KICH] to 246 in testicular germ cell tumors [TGCT], false discovery rate [FDR] <0.05, Figure 1B). These immune-related ERs were mainly involved in the "TCR Signaling Pathway" and "Antigen Processing and Presentation" across cancer types (Figure S1). Indeed, when deriving a general function of cellular component "APICAL_SURFACE" from Molecular Signature Database (MSigDB) as control, we found more ERs associated with the two pathways than control (p < 0.0001, Figure S1B). We ranked the ER-pathway pairs by their occurrence in 33 cancer types, and observed a complex relationship between ERs and immune pathways among the top 100 ER-pathway pairs, involving 31 ERs and 13 immune pathways (Figure 1C; Table S4). Noticeably, the most frequently identified pathways were "T cell receptor (TCR) Signaling Pathway" and "Antigen Pro-

cessing and Presentation," two key pathways involved in anti-tumor immune response regulation. For instance, the correlations between apolipoprotein B mRNA editing enzyme catalytic subunit 3H (APOBEC3H) and "Antigen Processing and Presentation" pathway were found in 25 cancers, consistent with previous studies that demonstrated APOBEC3H's associations with antigen processing and presentation, CD8 T cell infiltration and activation in cancer.[24,25] Chromatin reader speckled protein 140 (SP140), involved in diverse immune pathways in more than 10 cancer types, was reported to potentially control B cell development[26] and activity in cancer.[27]

To verify the ER-immune pathway relationships identified by EPRIM, we evaluated our findings in independent publicly available datasets of the same cancer type collected from the Gene Expression Omnibus (GEO). We found that the ER-immune pathway pairs identified in TCGA data were significantly enriched for those selected in the additional datasets for all cancer types (hypergeometric test, p value <0.001, Tables S5 and S6). When applied to artificial bulk profiles, calculated as the average expression of single cells grouped by patients (GSE72056 and GSE115978), we still observed a significant overlap (Table S5).

Identified ERs are associated with immune cell infiltration

Tumor-infiltrating immune cells exert vital roles in anti-tumor immune response. To investigate the correlations of identified ER expression with immune infiltrates, we obtained the infiltration abundances for six cell types (e.g., CD8 T cell) from the tumor immune estimation resource (TIMER).[28] We observed a high number of infiltration-related ERs across cancer types (spearman correlation, $|R| > 0.2$ and $p < 0.05$, Figure 2A; Table S7). For instance, in skin cutaneous melanoma (SKCM), 50% of immune ERs were related to CD8 T cell infiltration. A higher fraction of 57.41% was observed in stomach adenocarcinoma (STAD) for CD8 T cells. Interestingly, APOBEC3H and SP140, which we mentioned in the previous section, showed significant associations with CD8 T cells in more than 20 cancer types ($R > 0.5$ for STAD and $R > 0.4$ for SKCM, Figures S2A and S2B). Moreover, immune-related ERs tended to regulate immune infiltration in the majority of cancer types (Figures 2B–2D and S2C–S2E). In particular, strong correlations for the immune ERs were observed in SKCM and STAD upon CD8 T cells (Figure 2C, OR = 5.44, p = 1.92E−06 for SKCM and OR = 6.79, p = 1.46E−10 for STAD, Fisher's exact test). For example, the apolipoprotein B mRNA editing enzyme catalytic polypeptide-like 3 (APOBEC3) subfamily member apolipoprotein B mRNA editing enzyme catalytic subunit 3G (APOBEC3G) was correlated to CD8 T cell infiltration (Figure 2E), supported by a result identifying APOBEC3G as a potential biomarker of infiltrating T cells and improved patient clinical outcomes.[29] Growth factor independent 1 transcriptional repressor (GFI1) expression showed significant correlations with CD8 T cells (Figure 2F), consistent with previous reports demonstrating that GFI1 was correlated to infiltrating immune cells and played important roles in T cell polarization.[30,31] Moreover, Cell-type
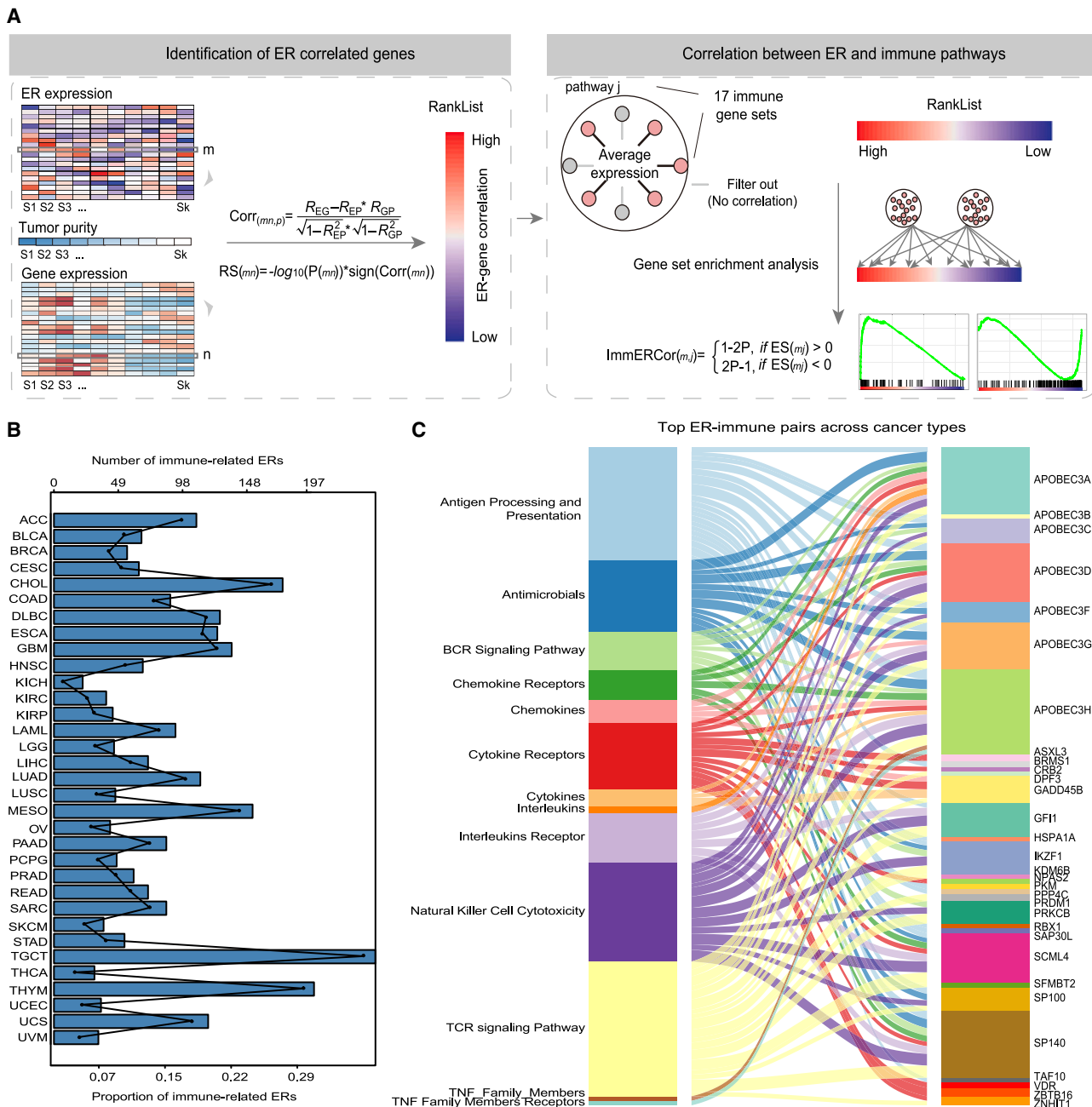
Figure 1. Identification of epigenetic regulators (ERs) related to immune pathways across cancer types
(A) Overview of the epigenetic regulator in immunology (EPRIM) method to capture the immune-related ERs. (B) The number (top x axis) and proportion (bottom x axis) of the immune-related ERs identified across 33 cancer types. (C) Alluvial diagram showing the top 100 ER-pathway association pairs across cancer types. The height of a stream field represents the number of occurrences in 33 cancer types.

Identification By Estimating Relative Subsets Of RNA Transcripts (CIBERSORT) that can estimate infiltration abundance of immune cells[32] identified infiltration-related ERs that were significantly over-lapped with those by TIMER (hypergeometric test, p values shown in Table S8). These results suggested that our identified immune-related ERs were potentially implicated in immune infiltration.

Identified immune ERs classify cancer patients with different survival
Given the associations with immune cell infiltration for the identified immune-related ERs, we further explored whether they contributed to the survival of cancer patients. As a result, significant associations between the expression of the identified ERs and cancer patients'
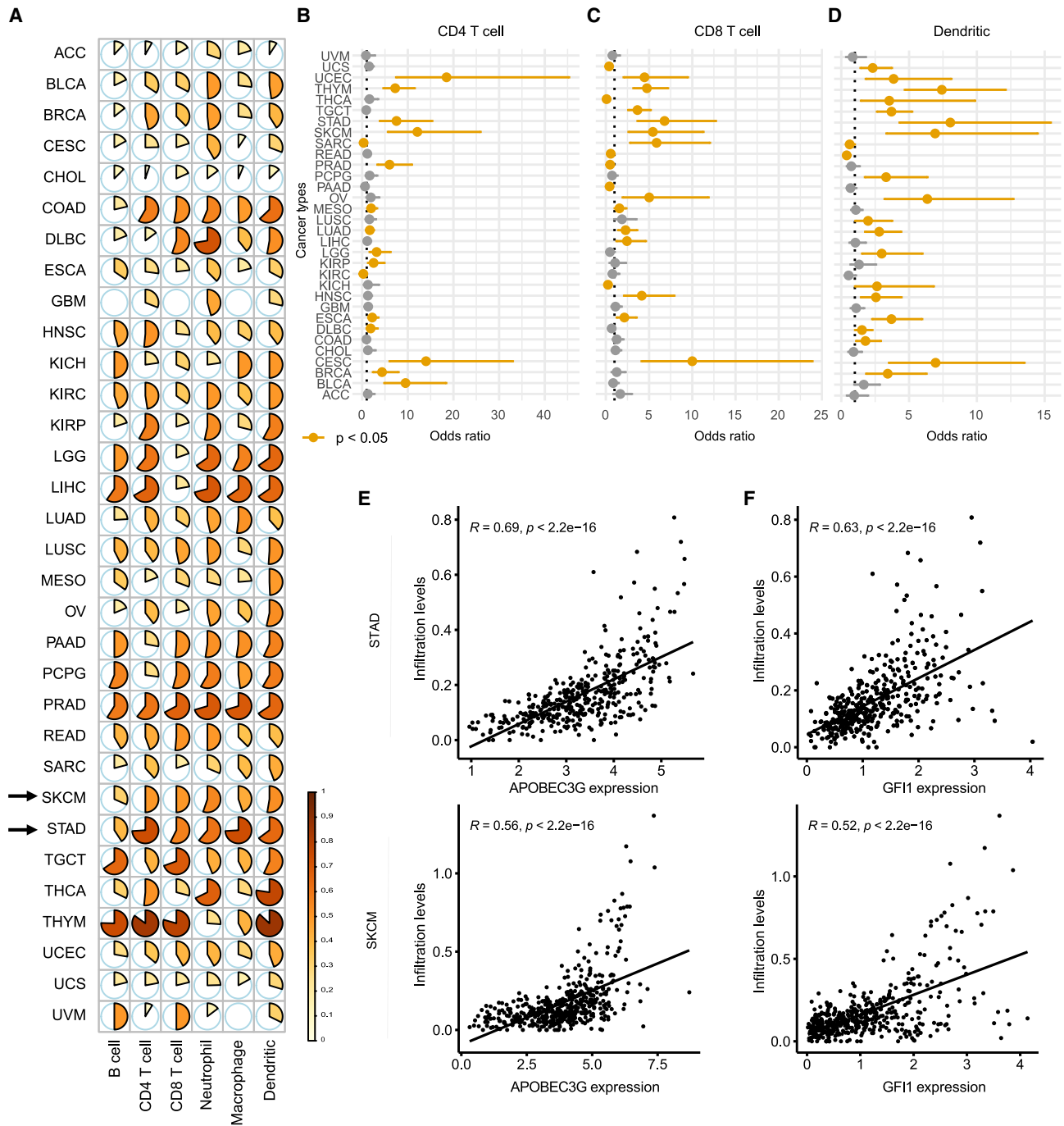
Figure 2. Associations between immune ERs and immune infiltrates in cancer

(A) The fraction of infiltration-related immune ERs upon different immune cells. (B–D) The odds ratios (dots) and 95% confidence intervals (lines) of the identified immune ERs upon infiltration-related ERs for immune cell types. Orange color indicates cancer types with p values <0.05. (E and F) Scatterplots showing the associations of estimated CD8 T cell abundance with expression levels of APOBEC3G (apolipoprotein B mRNA editing enzyme catalytic subunit 3G, E) and GFI1 (growth factor independent 1 transcriptional repressor, F). Spearman's correlations are indicated.
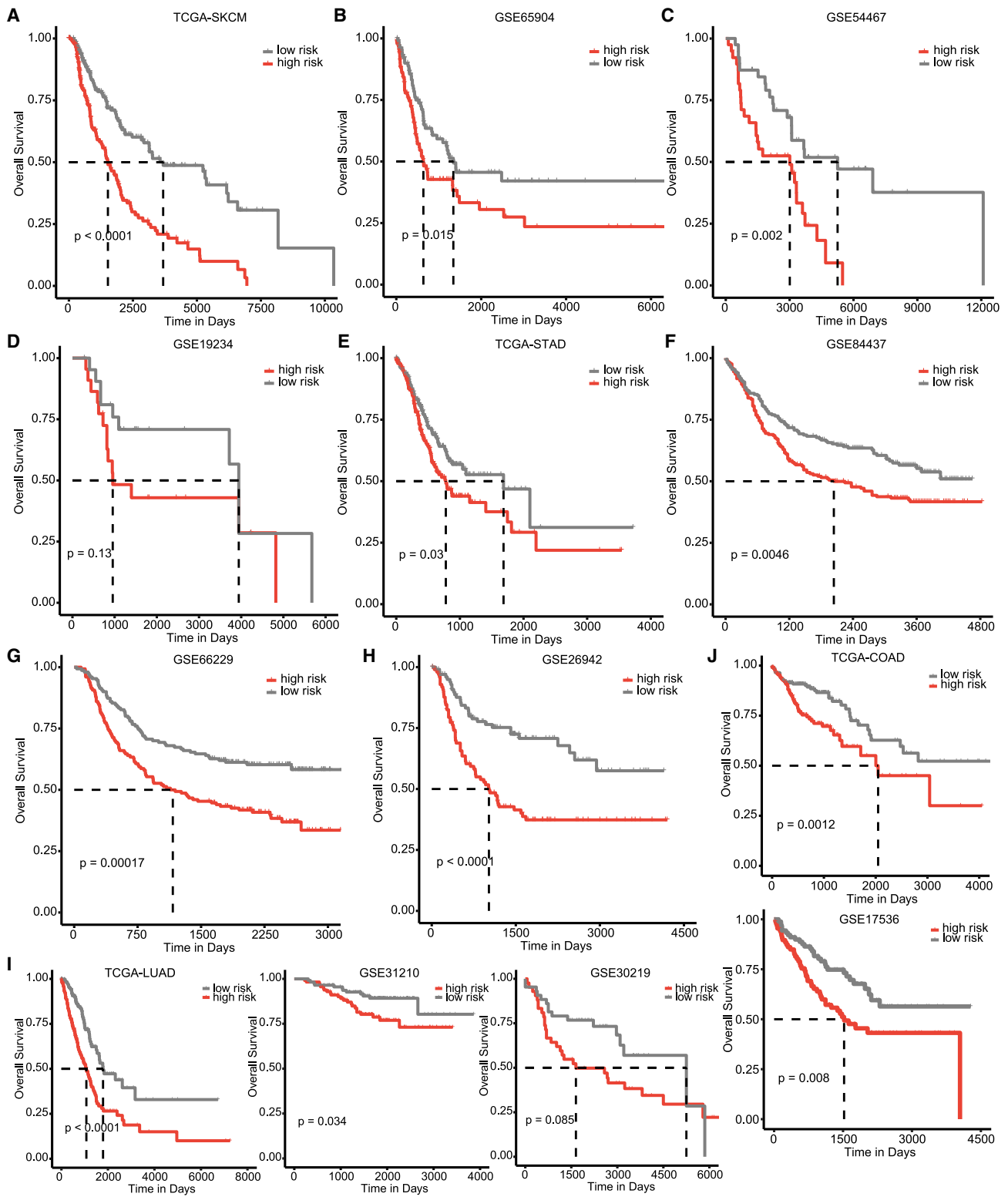
overall survival (OS) and progression-free survival (PFS) time were observed using univariate Cox proportional hazards regression for various cancers (Tables S9 and S10). Fourteen immune ERs showed significant associations with OS in SKCM, while a set of six and 24 prognostic ERs were identified in STAD and lung adenocarcinoma (LUAD), respectively.

We then constructed a prognostic signature using the expression of the OS-related ERs weighted by their Cox coefficients and finally obtained a risk score for each cancer patient. Using the median value of risk scores as a cutoff, two patient subgroups were obtained. We found significant associations between the risk signature and patient survival outcomes in multiple cancer types (Figures 3 and S3–S5). In SKCM, the high-risk patients showed obviously worse OS (hazard ratio [HR] = 1.202, 95% confidence interval [CI] = 1.131–1.277, log rank p < 0.0001) (Figure 3A; Table S11). Through multivariate Cox regression rectified by available factors containing age, gender, and tumor stage, the risk signature remained significant (p < 0.0001, Table S11). Receiver operating characteristic (ROC) evaluations demonstrated its predictive potential for OS at 1, 3, and 5 years (Figure S3A). Moreover, compared with other clinical factors, our signature showed a better discrimination for OS (Figures S3B–S3D). In three other independent data cohorts, the risk signature could also stratify patients into different risk groups with significant OS difference (Figures 3B–3D). The risk signature remained a prognostic potential regarding PFS (Figures S4A–S4D, S5A, and S5B; Table S12). Similar results were also observed for other cancers, including STAD, LUAD, and colon adenocarcinoma (COAD). In STAD, high-risk patients showed shorter OS and PFS (Figures 3E–3H, and S5E–S5G). Univariate and multivariate analyses collectively demonstrated the risk characteristic of ER-based signature indicating worse survival (p < 0.05, Tables S11 and S12). ROC analysis showed a superior accuracy of the risk signature than other standard clinical traits for patients' survival at 1, 3, and 5 years (Figures S3E–S3H, and S4E–S4H). Especially, in two independent datasets, survival analyses indicated a higher recurrence risk for high-risk patients (p < 0.01, Figures S5F and S5G). Survival curve analysis also showed the difference between patients stratified by the ER-based signature for patients' recurrence status (p < 0.05, Figures S5I and S5J) in LUAD. Taken together, these results demonstrated the power of the immune ER-defined risk signature used for stratifying patients with differential survival.

Distinct immune microenvironment and activity between immune ER-based subgroups
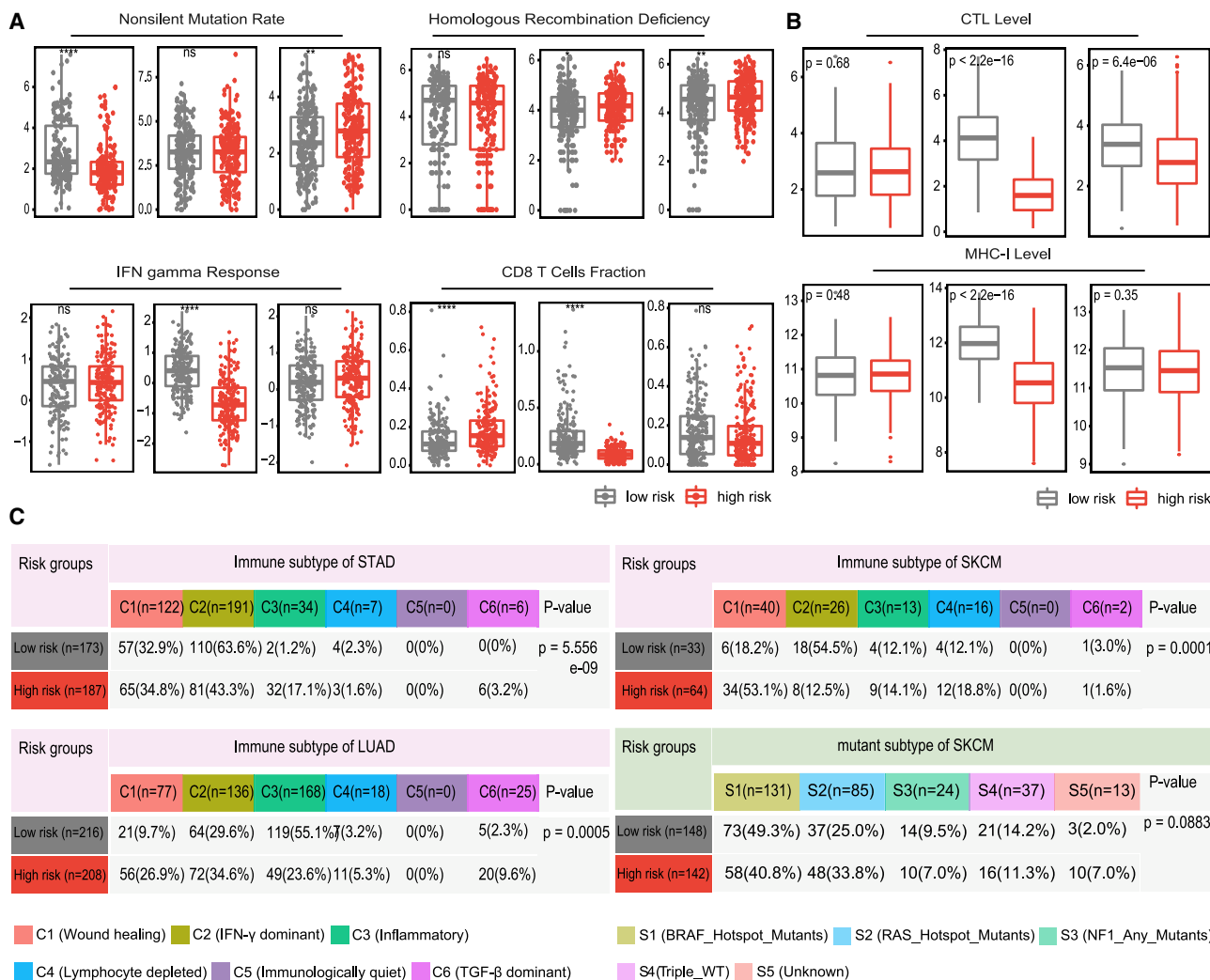
Tumor immune microenvironment (TIME) exerted the profound function for tumor initiation and development. To characterize the specific state of TIME in the two risk groups, we first investigated the immune characteristics obtained from Thorsson et al.[33] As determined by Wilcoxon's rank-sum test, we observed strong associations between our risk signature and some key immune functions regulating anti-tumor immune response in different cancer types. We found significantly higher DNA damage measures of homologous recombination deficiency (HRD) and copy number variation burden, tumor cell proliferation, and wound healing scores, while the lower lymphocyte infiltration signature scores, TCR diversity, interferon (IFN)-gamma and transforming growth factor (TGF)-beta response for high-risk patients of SKCM (p < 0.05, Figure 4A, and S6C). A study revealed the potential of HRD as an effective adjunct to enhance immunogenicity of tumors.[34] Similar results were also observed in LUAD (Figure 4A, and S6E). While, in STAD, we found an opposite distribution for high-risk patients (p < 0.05, Figures 4A and S6A). Cancer–immunity cycle depicted the biological processes in immune reaction and underlined the mechanisms for cancer–immunity interactions,[35] we also obtained the corresponding seven-step cycle scores of tumor samples (Figures S6B, S6D, and S6F).[36] In both SKCM and LUAD, patients with high risk scores showed suppressive immune activity with lower overall immune scores (Figures S6D and S6F) of steps 3–5, lower infiltration abundance of CD8 T and CD4 T cells measured by TIMER (Figures 4A, S6D, and S6F), lower levels of cytotoxic T cell infiltration and major histocompatibility complex class I (MHC-I) expression (p < 0.05, Figure 4B), while tumors with high risk scores in STAD had elevated immune cell abundance (Figures 4A and S6B).

Moreover, we investigated the distribution of six immune subtypes defined by immune signature sets.[33] In SKCM, the C1-wound healing subtype was enriched in the high-risk patient group, whereas the C2-interferon-gamma dominant subtype was mainly distributed in the patient group with low risk scores (Figure 4C). Compared with previously identified mutation-based molecular subtypes, the mutant RAS (mainly NRAS [NRAS proto-oncogene, GTPase]) subtype was dominant in the high-risk group, while the mutant B-Raf proto-oncogene, serine/threonine kinase (BRAF) subtype was dominant in the other subgroup (Figure 4C). For STAD, patients with high risk scores were enriched in the C6-TGF-beta dominant and C3-inflammatory subtypes; the C2-interferon-gamma dominant subtype was mainly associated with the patient group with low risk scores (Figure 4C), while we observed an opposite distribution in LUAD (Figure 4C). Taken together, these results demonstrated the different immune microenvironment and immune activity for the two ER-defined risk patient groups in different cancer types.

Figure 3. Prognostic associations of immune ER-based risk signature in cancer

(A–D) Kaplan-Meier curves showing overall survival (OS) according to the ER-based signature in TCGA-SKCM (The Cancer Genome Atlas-skin cutaneous melanoma) and other three independent datasets of melanoma. (E–H) Kaplan-Meier curves showing OS according to the ER-based signature in TCGA-STAD (stomach adenocarcinoma) and other three independent datasets of gastric cancer. (I) Kaplan-Meier curves showing OS according to the ER-based signature in TCGA-LUAD (lung adenocarcinoma) and other two independent datasets of lung cancer. (J) Kaplan-Meier curves showing OS according to the ER-based signature in TCGA-COAD (colon adenocarcinoma) and the other independent dataset of colon cancer.

A

Nonsilent Mutation Rate

Homologous Recombination Deficiency

B

CTL Level

MHC-I Level

IFN gamma Response

CD8 T Cells Fraction

low risk   high risk

low risk   high risk

C

Risk groups	Immune subtype of STAD						
	C1(n=122)	C2(n=191)	C3(n=34)	C4(n=7)	C5(n=0)	C6(n=6)	P-value
Low risk (n=173)	57(32.9%)	110(63.6%)	2(1.2%)	4(2.3%)	0(0%)	0(0%)	p = 5.556 e-09
High risk (n=187)	65(34.8%)	81(43.3%)	32(17.1%)	3(1.6%)	0(0%)	6(3.2%)	

Risk groups	Immune subtype of SKCM						
	C1(n=40)	C2(n=26)	C3(n=13)	C4(n=16)	C5(n=0)	C6(n=2)	P-value
Low risk (n=33)	6(18.2%)	18(54.5%)	4(12.1%)	4(12.1%)	0(0%)	1(3.0%)	p = 0.0001
High risk (n=64)	34(53.1%)	8(12.5%)	9(14.1%)	12(18.8%)	0(0%)	1(1.6%)	

Risk groups	Immune subtype of LUAD						
	C1(n=77)	C2(n=136)	C3(n=168)	C4(n=18)	C5(n=0)	C6(n=25)	P-value
Low risk (n=216)	21(9.7%)	64(29.6%)	119(55.1%)	7(3.2%)	0(0%)	5(2.3%)	p = 0.0005
High risk (n=208)	56(26.9%)	72(34.6%)	49(23.6%)	11(5.3%)	0(0%)	20(9.6%)	

Risk groups	mutant subtype of SKCM					
	S1(n=131)	S2(n=85)	S3(n=24)	S4(n=37)	S5(n=13)	P-value
Low risk (n=148)	73(49.3%)	37(25.0%)	14(9.5%)	21(14.2%)	3(2.0%)	p = 0.0883
High risk (n=142)	58(40.8%)	48(33.8%)	10(7.0%)	16(11.3%)	10(7.0%)	

C1 (Wound healing)   C2 (IFN-γ dominant)   C3 (Inflammatory)   S1 (BRAF_Hotspot_Mutants)   S2 (RAS_Hotspot_Mutants)   S3 (NF1_Any_Mutants)

C4 (Lymphocyte depleted)   C5 (Immunologically quiet)   C6 (TGF-β dominant)   S4(Triple_WT)   S5 (Unknown)

Figure 4. The immunological characterization of different patient groups
(A) Comparison of the nonsilent mutation rate, homologous recombination deficiency (HRD) score, interferon (IFN)-gamma response score and infiltration of CD8 T cells in two risk groups for STAD (left), SKCM (middle), and LUAD (right). (B) The distribution of cytotoxic T lymphocyte (CTL) levels and major histocompatibility complex class I (MHC-I) expression in two risk groups for STAD (left), SKCM (middle), and LUAD (right). (C) The association between risk groups with immune subtypes in STAD, SKCM, and LUAD. ns, non-significant, *p < 0.05, **p < 0.01, ***p < 0.001, and ****p < 0.0001.

Furthermore, we investigated the association of risk groups with mutations for cancer-specific driver genes[37] and found several significant associations (Figures S7A–S7C). For SKCM, BRAF had a higher mutation fraction in low-risk tumors, while NRAS had a higher mutation fraction in high-risk tumors (Figure S7B). For LUAD, the mutation rate in tumor protein p53 (TP53) was higher in high-risk tumors, while serine/threonine kinase 11 (STK11) driver gene was higher in low-risk tumors (Figure S7C). However, mutations in the selected driver genes including TP53, phosphatase and tensin homolog (PTEN), and phosphatidylinositol-4,5-bisphosphate 3-kinase catalytic subunit alpha (PIK3CA) were only enriched in low-risk tumors for STAD (Figure S7A).

An immune ER-based signature contributes to clinical outcomes from drug therapy

Given significant associations of risk groups with survival and immune activity, we next explored if the risk signature could predict immunotherapy response. Tumor immune dysfunction and exclusion (TIDE)[38] estimations quantifying the potential response of tumor samples to immune checkpoint blockade (ICB) were calculated. We noticed higher TIDE values for the high-risk patients and the estimated non-responders showed higher risk signature scores than the predicted responders (Figures 5A, 5E, S8A, and S8B), indicating that the high-risk patients were not inclined to gain ICB benefits.
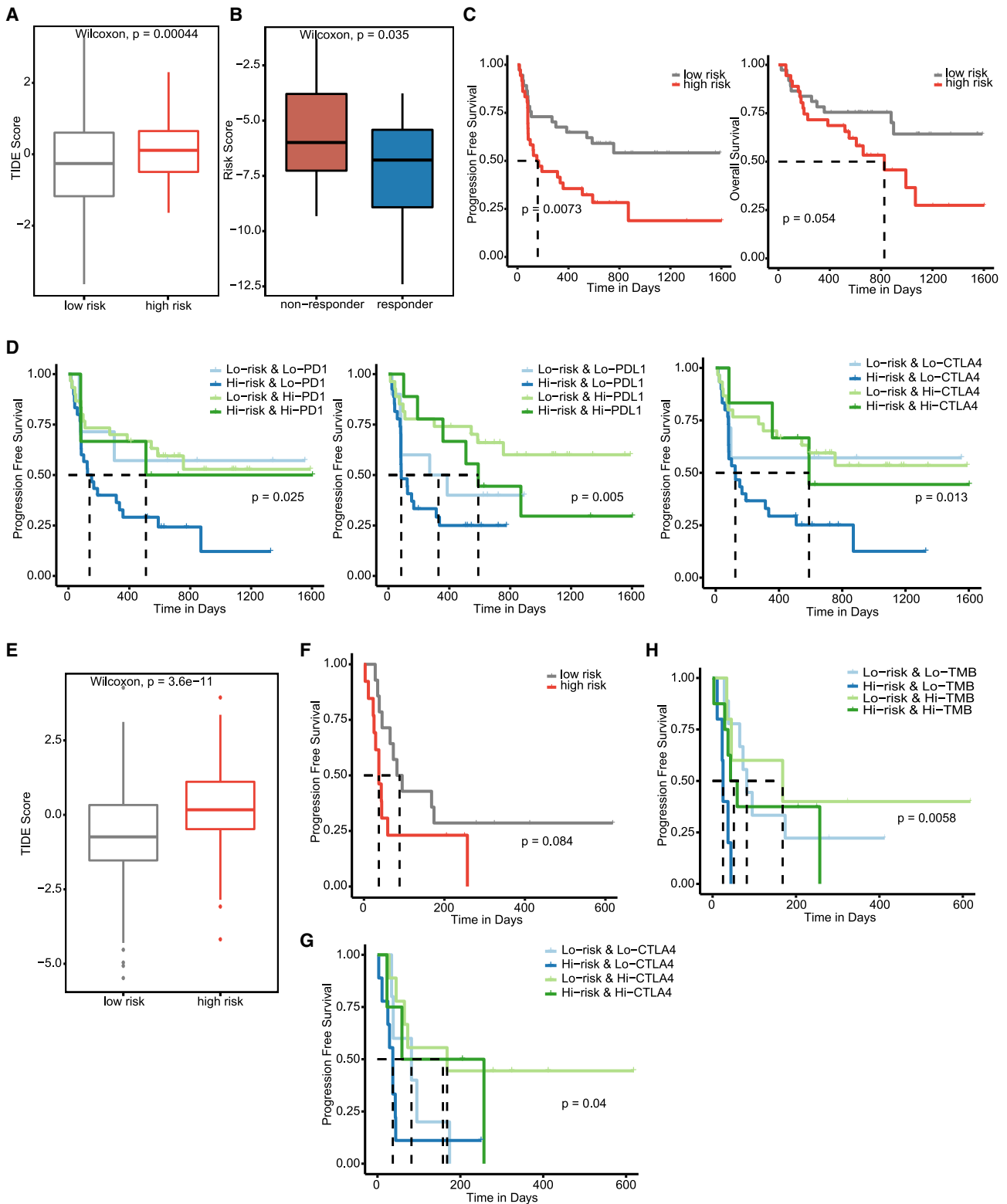
Based on an RNA-sequencing (RNA-seq) profile of melanoma samples receiving anti-PD1 (programmed death 1) or anti-CTLA4 (cytotoxic T-lymphocyte-associated protein 4) treatment (Gide cohort),[39] we calculated the risk scores of these samples using the risk signature model constructed with TCGA data (same Cox coefficients were used) and obtained two patient groups using the median value of risk scores as the cutoff. We noticed a significant association between our risk signature and the response to therapy (p < 0.05, Figure 5B). Patients with high risk scores showed dismal OS (HR = 2.075, 95% CI = 0.972–4.428, log rank p = 0.054) and PFS (HR = 2.318, 95% CI = 1.234–4.356, log rank p = 0.007). Multivariate regression analysis demonstrated the remaining association between our risk signature and patients' poor survival after adjusting for age and gender (p = 0.069 for OS and p = 0.011 for PFS, Figure 5C; Tables S13 and S14). Previous studies have demonstrated the improved clinical outcomes to ICB for patients with the expression of immune checkpoints,[40–42] especially inhibitory checkpoints PD1, programmed death-ligand 1 (PDL1), and CTLA4 expression. As expected, the patients with high risk scores showed lower expression for inhibitory checkpoints (p < 0.05 for PD1, PDL1, and CTLA4; Figure S8C). We further grouped the patients by checkpoint gene expression and our risk signature, using the median values as the cutoffs. The patients who were stratified into the high-risk and low-checkpoint groups showed a worse PFS and OS (Figures 5D and S8D). For the patients with high risk scores, survival differences were observed between low- and high-checkpoint groups (Figure 5D). For the patients with low checkpoint expression, we also observed noticeable survival differences between the two risk groups (Figure 5D). However, no survival difference was found regarding patients from the high-checkpoint group.

Similar results were also observed based on RNA-seq data for lung cancer samples receiving anti-PD1/PDL1 therapy (Jung cohort).[43] High-risk patients tended to show poorer PFS (Figure 5F). In multivariate analysis adjusting for age, gender, and mutation load, our risk signature remained associated with patients' poor survival (p = 0.008 for PFS, Figure 5F; Table S13). In addition, we found lower expression of checkpoint inhibitors for patients in the high-risk group (p = 0.012, p = 0.021 for PDL1 and CTLA4, respectively; Figure S8E). The patients from the high-risk group with low CTLA4 expression tended to have significantly worse PFS compared with other groups (p = 0.04, Figure 5G).

Tumor mutation burden (TMB) is the promising predictor regarding ICB, and high TMB usually indicates improved efficacy.[44,45] When stratifying the lung cancer patients with TMB and risk signature, significant survival disadvantages were found for the high-risk and low-TMB patients (p = 0.006, Figure 5H). Particularly, focusing on the low-TMB group only, the high-risk patients still showed poor PFS (log rank p = 0.007). These observations collectively indicated the predictive potential of ER-based risk signature for clinical survival outcomes of ICB therapy and highlighted its usefulness to further improve the patient stratification.

Compounds strongly correlated with risk scores can show therapeutic benefits. Using the Genomics of Drug Sensitivity in Cancer (GDSC)[46] platform, we evaluated whether our risk signature could predict drug sensitivity. Half maximal inhibitory concentration (IC50) values of the 198 compounds for each tumor sample were calculated across several cancer types. The spearman correlation analysis identified the candidate compounds for which drug sensitivity was positively associated with the risk signature (Figures 6A, 6D, 6G, and S9A), such as BMS-754807, SB-505124, and sepantronium bromide. High-risk patients showed lower IC50 for the selected compounds, indicating more drug sensitivity (Wilcoxon p < 0.001, Figures 6B, 6E, 6H, and S9B–S9D). We further annotated the signaling pathways and proteins targeted by these selected drugs and found that the drugs mainly targeted pathways including insulin-like growth factor 1 receptor (IGF1R) and phosphoinositide-3 kinase/mammalian target of rapamycin (PI3K/mTOR), cell cycle and extracellular signal-regulated kinase/mitogen-activated protein kinase (ERK/MAPK), apoptosis regulation signaling (Figures 6C, 6F, and 6I). The three most sensitive drugs BMS-754807, BI-2536, and sepantronium bromide targeted IGF1R, bromodomain containing 4 (BRD4), and survivin, respectively. Among the 13 compounds identified in STAD, BMS-754807 and JQ1 exhibited the strongest drug sensitivity with the most negative correlation coefficients (Figure 6A). BMS-754807 was previously shown to effectively inhibit the growth of gastric cancer[47] and epigenetic drug bromo and extra terminal (BET) inhibitor JQ1 could suppress the malignant progression of gastric cancer.[48–50] For SKCM (Figure 6D), previous studies focused on the efficacy of combination therapy with the selected drugs, namely SB-505124, trametinib, and ulixertinib, and other molecules.[51–54] For example, the combined delivery of TGF-beta inhibitor SB-505124 with interleukin (IL)-12 provided a valid immunotherapy in melanoma. A combination of trametinib and dabrafenib improved the clinical outcomes of melanoma. For LUAD (Figure 6G), the combination of the selected drug sepantronium bromide (survivin inhibitor) and other drugs exhibited a favorable safety profile in lung cancer treatment.[55,56] Taken together, our results underscored the utility of the immune ER-based signature in facilitating the treatment decision for cancer patients.

DISCUSSION

Epigenetic modifications are crucial in gene expression regulation and they could also modulate the immune microenvironment. Increasing

Figure 5. Association between immune ER-based signature and immune checkpoint blockade (ICB) response
(A) Differences of tumor immune dysfunction and exclusion (TIDE) scores for TCGA-SKCM. (B) Differences of risk scores for responders and non-responders of the melanoma patients received ICB. (C) Kaplan-Meier curves for progression-free and overall survival regarding the melanoma patients. (D) Survival analysis for progression-free survival regarding the melanoma patients grouped by risk signature and checkpoints. (E) Differences of the TIDE scores between risk groups for TCGA-LUAD. (F) Survival curves regarding progression-free survival for the lung cancer patients who received ICB therapy. (G and H) Kaplan-Meier analysis for progression-free survival regarding the lung cancer patient groups stratified by the risk signature and CTLA-4 (cytotoxic T-lymphocyte-associated protein 4, G) and TMB (tumor mutation burden, H).
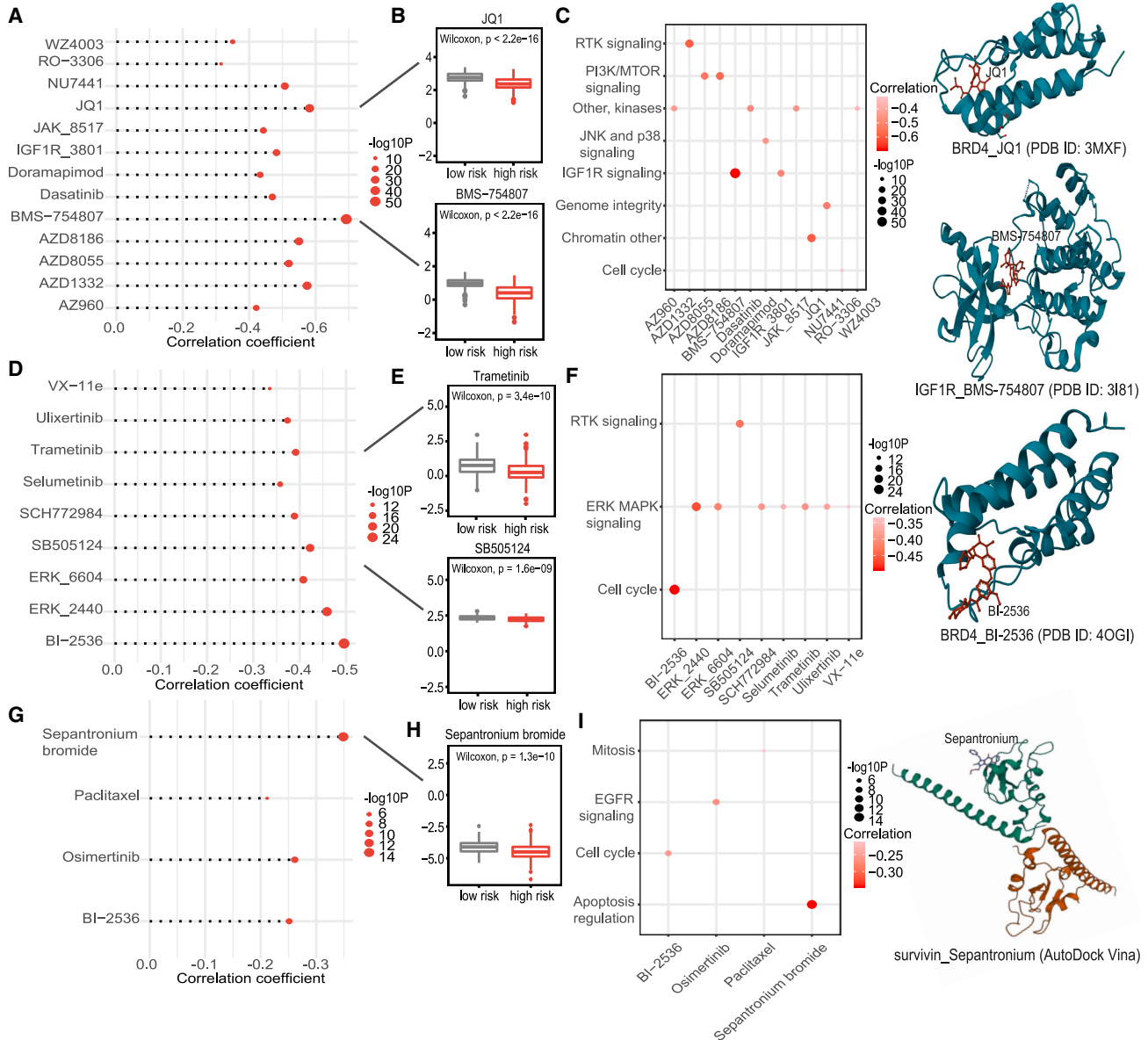
Figure 6. Evaluation of the correlation between drug sensitivity and risk signature

(A) Associations with the selected Genomics of Drug Sensitivity in Cancer (GDSC)-derived compounds in the STAD cohort. (B) Differences of the calculated half maximal inhibitory concentration (IC50) values (log-transformed). (C) Targeted signaling pathways (left) of the candidate compounds from GDSC database and the 3D interaction structure (right) with their target proteins. (D–F) The same as in (A–C), but for SKCM cohort. (G–I) The same as in (A–C), but for the LUAD cohort.

evidence demonstrates the role of ER genes in the immune system. However, few immune-related ERs were captured in tumor immune response. Therefore, an approach that aims to systematically identify immune-modulating ERs is still needed. In this study, we developed a dedicated approach, the epigenetic regulator in immunology (EPRIM), to identify immune-related ERs upon immunity-related pathways based on publicly available gene expression and immune profile data. We systematically identified immune-related ERs from 33 cancer types based on 17 immune pathways by using EPRIM.

To our best knowledge, it is the first dedicated tool that can fulfill the task. In addition, we provided the EPRIM-predicted results as a useful resource for the community. Besides, we revealed their potential roles in immune infiltration regulation. We successfully demonstrated their clinical relevance for predicting cancer prognosis and ICB response. Specifically, we established the ER-based risk model for prognosis and therapy response, and stratified cancer patients with different immunological characterization, highlighting their potential utility in clinical practice.

A successful immunotherapy largely depended on the knowledge on the function of immune system regarding cancer progression. Genetic or epigenetic determinants for dysregulated tumor immune microenvironment are still needed to fully explore. Emerging studies demonstrated that ERs were active participants in immune microenvironment modulation. However, the poor characterization for immune-related ERs in human tumors motivated us to study their roles in immune response. We designed an approach EPRIM that can systematically identify the ERs implicated in immune pathways. Using EPRIM, we presented the comprehensive landscape of associations between ER genes expression and 17 immune pathways at the first time. Across 33 cancer types, we found that ERs are not equally involved in these pathways, instead, they were mainly correlated to "TCR signaling pathway" and "antigen processing and presentation." TCR pathway is a well-known pathway that is important for the immune response,[57] which conducts the process of released antigen signal to T cells.[58] The immune-related ERs identified in this work were related to tumor immune infiltration, especially in SKCM and STAD. These observations underscored their potential importance in tumor immunology.

Previous reports have revealed the contribution of mutation to immune escape and resistance to immunotherapy.[59,60] Different mutation distribution of driver genes was shown (Figure S7). In SKCM, a higher mutation frequency of BRAF was observed for the low-risk group, while more frequent NRAS mutation was observed for high-risk group (Figure S7B). BRAF mutation was indicated to be associated with increased immune infiltration, while NRAS was the opposite.[61] One recent study characterized the crosstalk of tumor evolution with the immune system, demonstrating that early immune surveillance can confer a selection pressure with neoantigens depletion by promoter hypermethylation of genes harboring neoantigenic mutations, causing immune evasion.[62] This highlighted the importance of genetic and epigenetic regulation in tumor immune crosstalk and much more accurate mechanisms can be elucidated in the context of multi-omics data in further studies.

The immune ER-based signature identified by EPRIM also has clinical implications. In this work, we examined the effect of immune-related ERs on patient survival and constructed an ER-based risk model. Both worse overall and progress-free survival were observed for high-risk group in multiple independent datasets and cancer types (Figures 3 and S3–S5). Analyzing immune function and infiltration data, tumors with a higher risk score exhibited lower immune activity (Figures 4 and S6).

In addition, we also observed the association between ER-based risk signature and response to immunotherapy. A negative correlation regarding clinical outcomes for patients receiving immune checkpoint therapy was noticed (Figures 5A–5C, 5E, and 5F, S8A, and S8B). Moreover, we found notably lower expression values of immune checkpoints for high-risk patients (Figures S8C and S8E). When stratifying patients with the combination of our signature and checkpoint molecules, the worst sur-vivals were observed for the low-checkpoint and high-risk patients group (Figures 5D and 5G). The survival difference was observed for patient stratification by combining immune ER-based signature and TMB, helping the selection of patients with improved clinical benefits (Figure 5H). We further screened potential compounds used for high-risk patients, and found some promising compounds from the GDSC database, such as BMS-754807, SB-505124, and se-pantronium bromide (Figures 6 and S9), which mainly targeted pathways including IGF1R and PI3K/mTOR, cell cycle and ERK MAPK, and apoptosis regulation signaling pathways. Protein molecular interaction conformations supported the structural basis for BRD4_JQ1, IGF1R_BMS-754807, BRD4_BI-2536, and survivin_se-pantronium bromide (Figures 6C, 6F, and 6I), providing mechanistic clues to cure cancer. Pietro et al. evidenced the rationally designed polypharmacology for dual kinase-bromodomain inhibitor BI-2536, which targeted both the epigenetic reader domain of BRD4 and the kinase Polo-like kinase 1 (PLK1).[63] Interestingly, recent studies have reported the potentiated efficacy of ICB therapy by using the drugs by targeting ERs.[64,65] Consistently, the epigenetic drug JQ1, which was found to have high drug sensitivity for high-risk patients (Figures 6A–6C and S9A), could strengthen immune response through modulating T cell persistence.[66] Taken together, we demonstrated that the immune-related ERs may become promising targets by epi-drugs in combination with immunotherapy, augmenting anti-tumor effects.

In summary, the proposed algorithm EPRIM identified the ERs that had impact on immune pathways from pan-cancer and cancer-specific level. Our study also revealed the clinical potential of the identified immune-related ERs through the analysis of cancer patient survival and response to immunotherapy. The results shed new light on the understanding of ER function in immune regulation. The immune ERs therefore deserve to be further studied in mechanisms to develop and advance immunotherapy strategies and pharmaceuticals for human cancer.

MATERIALS AND METHODS
Acquisition of ERs
Human ER genes were collected from the previous studies,[22,67] which were annotated by "histone_type" or "methylator_type." A total of 690 ERs were included for the following analyses (Table S2).

Collection and refinement of immune gene sets
We acquired the signature gene sets of 17 immune pathways from ImmPort (https://www.immport.org/home),[23] which included immune categories of antimicrobials, cytokines, antigen processing, and presentation. The signature gene list and the pathway annotations used in our study are available in Table S3. Then, for each gene set, we computed the average expression and filtered genes by its expression correlation with the average. Spearman correlation was used, and we only retained significantly correlated genes ($p < 0.05$).

Molecular data

The mRNA expression profiles (TPM values, transcripts per kilobase million) of >10,000 tumor samples from TCGA across 33 cancers were downloaded (https://osf.io/gqrz9/wiki/home).[68] The cancer types and number of tumor samples are available in Table S1. We acquired clinical data of these samples and mutation data from the Pancancer Atlas consortium (https://gdc.cancer.gov/about-data/publications/pancanatlas). The cancer driver genes identified by a previous study were also used.[37]

Immune profile characterizing TCGA patients

The immune characteristics, published molecular subtypes, leukocyte fraction (LF), and CIBERSORT immune fractions for TCGA tumor samples were included from a previous study to measure the association between the risk signature and immune microenvironment.[33] We used immune fractions multiplying LF as absolute proportions for 22 immune cells in tumor tissue. We also obtained the estimated abundance of six infiltrating cells from TIMER (version 2.0, https://cistrome.shinyapps.io/timer), including CD8 T, CD4 T, B cells, neutrophils, macrophages, and dendritic cells. MHC-I and cytotoxic T lymphocyte (CTL) levels were measured by average gene expression according to previous literature. Genes HLA-A, HLA-B, HLA-C, and B2M were used to calculate the MHC-I expression level, while CD8A, CD8B, GZMA, GZMB, and PRF1 were used for CTL calculation.

EPRIM algorithm rationale

We proposed a computational algorithm EPRIM (Figure 1A) to identify ERs that were potentially involved in the immune function. In EPRIM, two types of data are mandatory: gene expression profiles of bulk samples as well as interested immune gene sets.

We first ranked the protein-coding genes (excluding ER genes) according to their expression correlation with a specific ER. Considering tumor purity was a confounding factor in the cancer gene expression analysis,[69,70] we then calculated the tumor purity of each sample through the ESTIMATE algorithm.[71] The numeric vectors representing ER m expression, and protein-coding gene n expression and tumor purity scores of samples from a specific cancer type were defined as $E(m) = (e_1, e_2, …, e_m, …, e_k)$, $G(n) = (g_1, g_2, …, g_n, …, g_k)$, and $P = (p_1, p_2, …, p_m, …, p_k)$, and the partial correlation coefficient (Corr) between ER m and protein-coding gene n correcting for purity was defined as follows:

$$Corr(mn) = \frac{R_{EG} - R_{EP} * R_{GP}}{\sqrt{1 - R_{EP}^2} * \sqrt{1 - R_{GP}^2}}$$

R_{EG} represents the coefficient for ER m and protein-coding gene n, R_{EP} represents the coefficient for ER m and tumor purity, and R_{GP} represents the coefficient for protein-coding gene n and tumor purity. By combing Corr and p value of the Corr (P(mn)) for each ER-coding gene pair, the protein-coding genes were ranked by the RS regarding each ER.

$$RS(mn) = - log_{10}(P(mn)) * sign(Corr(mn))$$

Then, for each gene set in 17 immune-related pathways, we conducted gene set enrichment analysis (GSEA)[21] for quantifying expression shift of immune genes (fgsea package, version 1.24.0). In brief, by moving from the top to bottom of the ranked gene list one by one, we computed two types of weighted gene fractions through determining if they were immune genes at each step. One type was the fraction of genes in one immune pathway ("hits") weighted by their rank scores and the other was the fraction of genes not in this pathway ("misses"). For each ER-pathway pair, the enrichment score (ES) and p value were obtained. We selected the significant ER-immune pairs with false discovery rate (FDR) < 0.05. A correlation score ImmERCor between ER m and immune pathway j was defined as follows:

$$ImmERCor(m, j) = \begin{cases} 1 - 2p, if\ ES(mj) > 0 \\ 2p - 1, if\ ES(mj) < 0 \end{cases}$$

Construction of a prognostic immune ER signature

To investigate the clinical correlation of immune-related ERs, we established an ER-based signature. By univariate Cox regression analysis, the immune ERs significantly correlated with patients' OS were retained (p < 0.05). Then for each patient, we computed a risk signature score by weighted sum expression: $riskscore = \sum_{i=1}^{n} coef(ER_i) * exp(ER_i)$, where coef($ER_i$) and exp($ER_i$) indicate the Cox coefficients and expression levels for the ith ER, respectively. Using the median value of risk scores as the cutoff, the patients of a cancer type were grouped into high- and low-risk subgroups.

Estimation of drug sensitivity

We acquired the drug response data against cancer cell lines from GDSC (https://www.cancerrxgene.org),[46] where the drug sensitivity information with IC50 value was available (lower level points to a stronger response). Transcriptome data for cancer cell lines were also used.[72] For drug response prediction, the gene expression and response data of cancer cell lines from GDSC2 provided by the oncoPredict OSF (https://osf.io/c6tfx) were used as the training data, and the TCGA gene expression data of a specific cancer type as the testing data. For each patient of a cancer type, we estimated the IC50 value of each compound via oncoPredict package (version 0.2).[73] TIDE web application was used for evaluating the potential response of patients to ICB based on the gene expression profile of a specific cancer type (http://tide.dfci.harvard.edu).[38]

Statistical analysis

Two-sided Wilcoxon rank-sum test was conducted for comparing feature values between two patient groups. Spearman correlation coefficient was calculated to measure the associations between two variables. Associations between variables and survivals were tested using univariate/multivariate Cox proportional hazard regression (survival package, version 3.5.0), and the survival comparison by log rank test was then conducted. ROC curves were generated by the pROC

package (version 1.18.0). The time-dependent areas under the curve were drawn via the timeROC package (version 0.4). All statistical analyses and the main algorithm were run in R computing system version 4.2.0.

DATA AND CODE AVAILABILITY

The data analyzed in this study are available in the article or from the authors upon reasonable request. The open-source codes of EPRIM can be found at https://github.com/syy2017/EPRIM.

SUPPLEMENTAL INFORMATION

Supplemental information can be found online at https://doi.org/10.1016/j.omtn.2023.102100.

AUTHOR CONTRIBUTIONS

J.L. and J.Z. conceived, designed, and supervised the study; A.S., C.L., Y.C., and J.W. collected data; A.S. and C.L. performed analysis and data interpretation; A.S. wrote the manuscript; A.S., J.W., Y.C., J.Z., and J.L. commented on and revised the manuscript. All authors read and approved the final manuscript.

DECLARATION OF INTERESTS

The authors declare no competing interests.

REFERENCES

1. Kaufmann, S.H.E. (2019). Immunology's Coming of Age. Front. Immunol. 10, 684.

2. Egen, J.G., Ouyang, W., and Wu, L.C. (2020). Human Anti-tumor Immunity: Insights from Immunotherapy Clinical Trials. Immunity 52, 36–54.

3. O'Donnell, J.S., Teng, M.W.L., and Smyth, M.J. (2019). Cancer immunoediting and resistance to T cell-based immunotherapy. Nat. Rev. Clin. Oncol. 16, 151–167.

4. Rodig, S.J., Gusenleitner, D., Jackson, D.G., Gjini, E., Giobbie-Hurder, A., Jin, C., Chang, H., Lovitch, S.B., Horak, C., Weber, J.S., et al. (2018). MHC proteins confer differential sensitivity to CTLA-4 and PD-1 blockade in untreated metastatic melanoma. Sci. Transl. Med. 10, eaar3342.

5. Jhunjhunwala, S., Hammer, C., and Delamarre, L. (2021). Antigen presentation in cancer: insights into tumour immunogenicity and immune evasion. Nat. Rev. Cancer 21, 298–312.

6. Dawson, M.A., and Kouzarides, T. (2012). Cancer epigenetics: from mechanism to therapy. Cell 150, 12–27.

7. Goldberg, A.D., Allis, C.D., and Bernstein, E. (2007). Epigenetics: a landscape takes shape. Cell 128, 635–638.

8. Garcia-Martinez, L., Zhang, Y., Nakata, Y., Chan, H.L., and Morey, L. (2021). Epigenetic mechanisms in breast cancer therapy and resistance. Nat. Commun. 12, 1786.

9. Berglund, A., Mills, M., Putney, R.M., Hamaidi, I., Mulé, J., and Kim, S. (2020). Methylation of immune synapse genes modulates tumor immunogenicity. J. Clin. Invest. 130, 974–980.

10. Chen, T., and Dent, S.Y.R. (2014). Chromatin modifiers and remodellers: regulators of cellular differentiation. Nat. Rev. Genet. 15, 93–106.

11. Bell, O., Tiwari, V.K., Thomä, N.H., and Schübeler, D. (2011). Determinants and dynamics of genome accessibility. Nat. Rev. Genet. 12, 554–564.

12. Rodrigues, C.P., Shvedunova, M., and Akhtar, A. (2021). Epigenetic Regulators as the Gatekeepers of Hematopoiesis. Trends Genet. 37, 125–142.

13. Halaburkova, A., Cahais, V., Novoloaca, A., Araujo, M.G.d.S., Khoueiry, R., Ghantous, A., and Herceg, Z. (2020). Pan-cancer multi-omics analysis and orthogonal experimental assessment of epigenetic driver genes. Genome Res. 30, 1517–1532.

14. Alipour, M., Sheikhnejad, R., Fouani, M.H., Bardania, H., and Hosseinkhani, S. (2023). DNAi-peptide nanohybrid smart particles target BCL-2 oncogene and induce apoptosis in breast cancer cells. Biomed. Pharmacother. 166, 115299.

15. Alipour, M., Javeshghani, D., and Roustazadeh, A. (2022). Gene expression pattern in severely progressing covid-19 patients is related to diabetes mellitus type 1. A functional annotation analysis 33, 201039.

16. Duan, Q., Zhang, H., Zheng, J., and Zhang, L. (2020). Turning Cold into Hot: Firing up the Tumor Microenvironment. Trends Cancer 6, 605–618.

17. Wang, G., Yang, L., Gao, J., Mu, H., Song, Y., Jiang, X., Chen, B., and Cui, R. (2021). Identification of Candidate Biomarker ASXL2 and Its Predictive Value in Pancreatic Carcinoma. Front. Oncol. 11, 736694.

18. Zhang, M., Liu, Z.Z., Aoshima, K., Cai, W.L., Sun, H., Xu, T., Zhang, Y., An, Y., Chen, J.F., Chan, L.H., et al. (2022). CECR2 drives breast cancer metastasis by promoting NF-kappaB signaling and macrophage-mediated immune suppression. Sci. Transl. Med. 14, eabf5473.

19. Li, J., Yuan, S., Norgard, R.J., Yan, F., Sun, Y.H., Kim, I.K., Merrell, A.J., Sela, Y., Jiang, Y., Bhanu, N.V., et al. (2021). Epigenetic and Transcriptional Control of the Epidermal Growth Factor Receptor Regulates the Tumor Immune Microenvironment in Pancreatic Cancer. Cancer Discov. 11, 736–753.

20. Cai, J., Wu, S., Zhang, F., and Dai, Z. (2022). Construction and Validation of an Epigenetic Regulator Signature as A Novel Biomarker For Prognosis, Immunotherapy, And Chemotherapy In Hepatocellular Carcinoma. Front. Immunol. 13, 952413.

21. Subramanian, A., Tamayo, P., Mootha, V.K., Mukherjee, S., Ebert, B.L., Gillette, M.A., Paulovich, A., Pomeroy, S.L., Golub, T.R., Lander, E.S., and Mesirov, J.P. (2005). Gene set enrichment analysis: a knowledge-based approach for interpreting genome-wide expression profiles. Proc. Natl. Acad. Sci. USA. 102, 15545–15550.

22. Lu, J., Xu, J., Li, J., Pan, T., Bai, J., Wang, L., Jin, X., Lin, X., Zhang, Y., Li, Y., et al. (2018). FACER: comprehensive molecular and functional characterization of epigenetic chromatin regulators. Nucleic Acids Res. 46, 10019–10033.

23. Bhattacharya, S., Dunn, P., Thomas, C.G., Smith, B., Schaefer, H., Chen, J., Hu, Z., Zalocusky, K.A., Shankar, R.D., Shen-Orr, S.S., et al. (2018). ImmPort, toward repurposing of open access immunological assay data for translational and clinical research. Sci. Data 5, 180015.

24. Granadillo Rodríguez, M., Flath, B., and Chelico, L. (2020). The interesting relationship between APOBEC3 deoxycytidine deaminases and cancer: a long road ahead. Open Biol. 10, 200188.

25. Liu, Q., Luo, Y.W., Cao, R.Y., Pan, X., Chen, X.J., Zhang, S.Y., Zhang, W.L., Zhou, J.Y., Cheng, B., and Ren, X.Y. (2020). Association between APOBEC3H-Mediated Demethylation and Immune Landscape in Head and Neck Squamous Carcinoma. BioMed Res. Int. 2020, 4612375.

26. Fraschilla, I., and Jeffrey, K.L. (2020). The Speckled Protein (SP) Family: Immunity's Chromatin Readers. Trends Immunol. 41, 572–585.

27. Weiner, A.B., Yu, C.Y., Kini, M., Liu, Y., Davicioni, E., Mitrofanova, A., Lotan, T.L., and Schaeffer, E.M. (2023). High intratumoral plasma cells content in primary prostate cancer defines a subset of tumors with potential susceptibility to immune-based treatments. Prostate Cancer Prostatic Dis. 26, 105–112.

28. Li, T., Fan, J., Wang, B., Traugh, N., Chen, Q., Liu, J.S., Li, B., and Liu, X.S. (2017). TIMER: A Web Server for Comprehensive Analysis of Tumor-Infiltrating Immune Cells. Cancer Res. 77, e108–e110.

29. Leonard, B., Starrett, G.J., Maurer, M.J., Oberg, A.L., Van Bockstal, M., Van Dorpe, J., De Wever, O., Helleman, J., Sieuwerts, A.M., Berns, E.M.J.J., et al. (2016). APOBEC3G Expression Correlates with T-Cell Infiltration and Improved Clinical

Outcomes in High-grade Serous Ovarian Carcinoma. Clin. Cancer Res. *22*, 4746–4755.

30. Zhou, B., Yu, J., Cai, X., and Wu, S. (2022). Constructing a molecular subtype model of colon cancer using machine learning. Front. Pharmacol. *13*, 1008207.

31. Friesen, L., Kostlan, R., Liu, Q., Yu, H., Zhu, J., Lukacs, N., and Kim, C.H. (2022). Cutting Edge: The Expression of Transcription Inhibitor GFI1 Is Induced by Retinoic Acid to Rein in Th9 Polarization. J. Immunol. *209*, 1237–1242.

32. Newman, A.M., Liu, C.L., Green, M.R., Gentles, A.J., Feng, W., Xu, Y., Hoang, C.D., Diehn, M., and Alizadeh, A.A. (2015). Robust enumeration of cell subsets from tissue expression profiles. Nat. Methods *12*, 453–457.

33. Thorsson, V., Gibbs, D.L., Brown, S.D., Wolf, D., Bortone, D.S., Ou Yang, T.H., Porta-Pardo, E., Gao, G.F., Plaisier, C.L., Eddy, J.A., et al. (2019). The Immune Landscape of Cancer. Immunity *51*, 411–412.

34. Telli, M.L., Stover, D.G., Loi, S., Aparicio, S., Carey, L.A., Domchek, S.M., Newman, L., Sledge, G.W., and Winer, E.P. (2018). Homologous recombination deficiency and host anti-tumor immunity in triple-negative breast cancer. Breast Cancer Res. Treat. *171*, 21–31.

35. Chen, D.S., and Mellman, I. (2013). Oncology meets immunology: the cancer-immunity cycle. Immunity *39*, 1–10.

36. Xu, L., Deng, C., Pang, B., Zhang, X., Liu, W., Liao, G., Yuan, H., Cheng, P., Li, F., Long, Z., et al. (2018). TIP: A Web Server for Resolving Tumor Immunophenotype Profiling. Cancer Res. *78*, 6575–6580.

37. Bailey, M.H., Tokheim, C., Porta-Pardo, E., Sengupta, S., Bertrand, D., Weerasinghe, A., Colaprico, A., Wendl, M.C., Kim, J., Reardon, B., et al. (2018). Comprehensive Characterization of Cancer Driver Genes and Mutations. Cell *174*, 1034–1035.

38. Jiang, P., Gu, S., Pan, D., Fu, J., Sahu, A., Hu, X., Li, Z., Traugh, N., Bu, X., Li, B., et al. (2018). Signatures of T cell dysfunction and exclusion predict cancer immunotherapy response. Nat. Med. *24*, 1550–1558.

39. Gide, T.N., Quek, C., Menzies, A.M., Tasker, A.T., Shang, P., Holst, J., Madore, J., Lim, S.Y., Velickovic, R., Wongchenko, M., et al. (2019). Distinct Immune Cell Populations Define Response to Anti-PD-1 Monotherapy and Anti-PD-1/Anti-CTLA-4 Combined Therapy. Cancer Cell *35*, 238–255.e6.

40. Taube, J.M., Klein, A., Brahmer, J.R., Xu, H., Pan, X., Kim, J.H., Chen, L., Pardoll, D.M., Topalian, S.L., and Anders, R.A. (2014). Association of PD-1, PD-1 ligands, and other features of the tumor immune microenvironment with response to anti-PD-1 therapy. Clin. Cancer Res. *20*, 5064–5074.

41. Daud, A.I., Wolchok, J.D., Robert, C., Hwu, W.J., Weber, J.S., Ribas, A., Hodi, F.S., Joshua, A.M., Kefford, R., Hersey, P., et al. (2016). Programmed Death-Ligand 1 Expression and Response to the Anti-Programmed Death 1 Antibody Pembrolizumab in Melanoma. J. Clin. Oncol. *34*, 4102–4109.

42. Herbst, R.S., Soria, J.C., Kowanetz, M., Fine, G.D., Hamid, O., Gordon, M.S., Sosman, J.A., McDermott, D.F., Powderly, J.D., Gettinger, S.N., et al. (2014). Predictive correlates of response to the anti-PD-L1 antibody MPDL3280A in cancer patients. Nature *515*, 563–567.

43. Jung, H., Kim, H.S., Kim, J.Y., Sun, J.M., Ahn, J.S., Ahn, M.J., Park, K., Esteller, M., Lee, S.H., and Choi, J.K. (2019). DNA methylation loss promotes immune evasion of tumours with high mutation and copy number load. Nat. Commun. *10*, 4278.

44. Rizvi, H., Sanchez-Vega, F., La, K., Chatila, W., Jonsson, P., Halpenny, D., Plodkowski, A., Long, N., Sauter, J.L., Rekhtman, N., et al. (2018). Molecular Determinants of Response to Anti-Programmed Cell Death (PD)-1 and Anti-Programmed Death-Ligand 1 (PD-L1) Blockade in Patients With Non-Small-Cell Lung Cancer Profiled With Targeted Next-Generation Sequencing. J. Clin. Oncol. *36*, 633–641.

45. Chan, T.A., Yarchoan, M., Jaffee, E., Swanton, C., Quezada, S.A., Stenzinger, A., and Peters, S. (2019). Development of tumor mutation burden as an immunotherapy biomarker: utility for the oncology clinic. Ann. Oncol. *30*, 44–56.

46. Yang, W., Soares, J., Greninger, P., Edelman, E.J., Lightfoot, H., Forbes, S., Bindal, N., Beare, D., Smith, J.A., Thompson, I.R., et al. (2013). Genomics of Drug Sensitivity in Cancer (GDSC): a resource for therapeutic biomarker discovery in cancer cells. Nucleic Acids Res. *41*, D955–D961.

47. Carboni, J.M., Wittman, M., Yang, Z., Lee, F., Greer, A., Hurlburt, W., Hillerman, S., Cao, C., Cantor, G.H., Dell-John, J., et al. (2009). BMS-754807, a small molecule inhibitor of insulin-like growth factor-1R/IR. Mol. Cancer Ther. *8*, 3341–3349.

48. Zhou, S., Zhang, S., Wang, L., Huang, S., Yuan, Y., Yang, J., Wang, H., Li, X., Wang, P., Zhou, L., et al. (2020). BET protein inhibitor JQ1 downregulates chromatin accessibility and suppresses metastasis of gastric cancer via inactivating RUNX2/NID1 signaling. Oncogenesis *9*, 33.

49. Dong, X., Hu, X., Chen, J., Hu, D., and Chen, L.F. (2018). BRD4 regulates cellular senescence in gastric cancer cells via E2F/miR-106b/p21 axis. Cell Death Dis. *9*, 203.

50. Montenegro, R.C., Clark, P.G.K., Howarth, A., Wan, X., Ceroni, A., Siejka, P., Nunez-Alonso, G.A., Monteiro, O., Rogers, C., Gamble, V., et al. (2016). BET inhibition as a new strategy for the treatment of gastric cancer. Oncotarget *7*, 43997–44012.

51. Jiang, J., Zhang, Y., Peng, K., Wang, Q., Hong, X., Li, H., Fan, G., Zhang, Z., Gong, T., and Sun, X. (2017). Combined delivery of a TGF-beta inhibitor and an adenoviral vector expressing interleukin-12 potentiates cancer immunotherapy. Acta Biomater. *61*, 114–123.

52. Long, G.V., Stroyakovskiy, D., Gogas, H., Levchenko, E., de Braud, F., Larkin, J., Garbe, C., Jouary, T., Hauschild, A., Grob, J.J., et al. (2014). Combined BRAF and MEK inhibition versus BRAF inhibition alone in melanoma. N. Engl. J. Med. *371*, 1877–1888.

53. Wolfe, Z., Friedland, J.C., Ginn, S., Blackham, A., Demberger, L., Horton, M., McIntosh, A., Sheikh, H., Box, J., Knorzer, D., et al. (2022). Case report: response to the ERK1/2 inhibitor ulixertinib in BRAF D594G cutaneous melanoma. Melanoma Res. *32*, 295–298.

54. Germann, U.A., Furey, B.F., Markland, W., Hoover, R.R., Aronov, A.M., Roix, J.J., Hale, M., Boucher, D.M., Sorrell, D.A., Martinez-Botella, G., et al. (2017). Targeting the MAPK Signaling Pathway in Cancer: Promising Preclinical Activity with the Novel Selective ERK1/2 Inhibitor BVD-523 (Ulixertinib). Mol. Cancer Ther. *16*, 2351–2363.

55. Başpınar, Y., Erel-Akbaba, G., Kotmakçı, M., and Akbaba, H. (2019). Development and characterization of nanobubbles containing paclitaxel and survivin inhibitor YM155 against lung cancer. Int. J. Pharm. *566*, 149–156.

56. Kelly, R.J., Thomas, A., Rajan, A., Chun, G., Lopez-Chavez, A., Szabo, E., Spencer, S., Carter, C.A., Guha, U., Khozin, S., et al. (2013). A phase I/II study of sepantronium bromide (YM155, survivin suppressor) with paclitaxel and carboplatin in patients with advanced non-small-cell lung cancer. Ann. Oncol. *24*, 2601–2606.

57. Ma, J.M., Cui, Y.X., Ge, X., Li, J., Li, J.R., and Wang, X.N. (2015). Association of TCR-signaling pathway with the development of lacrimal gland benign lymphoepithelial lesions. Int. J. Ophthalmol. *8*, 685–689.

58. Zeng, L., Palaia, I., Šarić, A., and Su, X. (2021). PLCgamma1 promotes phase separation of T cell signaling components. J. Cell Biol. *220*, e202009154.

59. Liao, W., Overman, M.J., Boutin, A.T., Shang, X., Zhao, D., Dey, P., Li, J., Wang, G., Lan, Z., Li, J., et al. (2019). KRAS-IRF2 Axis Drives Immune Suppression and Immune Therapy Resistance in Colorectal Cancer. Cancer Cell *35*, 559–572.e7.

60. Zaretsky, J.M., Garcia-Diaz, A., Shin, D.S., Escuin-Ordinas, H., Hugo, W., Hu-Lieskovan, S., Torrejon, D.Y., Abril-Rodriguez, G., Sandoval, S., Barthly, L., et al. (2016). Mutations Associated with Acquired Resistance to PD-1 Blockade in Melanoma. N. Engl. J. Med. *375*, 819–829.

61. Xu, L., Zhu, S., Lan, Y., Yan, M., Jiang, Z., Zhu, J., Liao, G., Ping, Y., Xu, J., Pang, B., et al. (2022). Revealing the contribution of somatic gene mutations to shaping tumor immune microenvironment. Brief. Bioinform. *23*, bbac064.

62. Rosenthal, R., Cadieux, E.L., Salgado, R., Bakir, M.A., Moore, D.A., Hiley, C.T., Lund, T., Tanić, M., Reading, J.L., Joshi, K., et al. (2019). Neoantigen-directed immune escape in lung cancer evolution. Nature *567*, 479–485.

63. Ciceri, P., Müller, S., O'Mahony, A., Fedorov, O., Filippakopoulos, P., Hunt, J.P., Lasater, E.A., Pallares, G., Picaud, S., Wells, C., et al. (2014). Dual kinase-bromodomain inhibitors for rationally designed polypharmacology. Nat. Chem. Biol. *10*, 305–312.

64. Ghoneim, H.E., Fan, Y., Moustaki, A., Abdelsamed, H.A., Dash, P., Dogra, P., Carter, R., Awad, W., Neale, G., Thomas, P.G., and Youngblood, B. (2017). De Novo Epigenetic Programs Inhibit PD-1 Blockade-Mediated T Cell Rejuvenation. Cell *170*, 142–157.e19.

65. Llopiz, D., Ruiz, M., Villanueva, L., Iglesias, T., Silva, L., Egea, J., Lasarte, J.J., Pivette, P., Trochon-Joseph, V., Vasseur, B., et al. (2019). Enhanced anti-tumor efficacy of checkpoint inhibitors in combination with the histone deacetylase inhibitor Belinostat in a murine hepatocellular carcinoma model. Cancer Immunol. Immunother. *68*, 379–393.

66. Zhu, H., Bengsch, F., Svoronos, N., Rutkowski, M.R., Bitler, B.G., Allegrezza, M.J., Yokoyama, Y., Kossenkov, A.V., Bradner, J.E., Conejo-Garcia, J.R., and Zhang, R. (2016). BET Bromodomain Inhibition Promotes Anti-tumor Immunity by Suppressing PD-L1 Expression. Cell Rep. *16*, 2829–2837.

67. Wang, J., Shi, A., and Lyu, J. (2023). A comprehensive atlas of epigenetic regulators reveals tissue-specific epigenetic regulation patterns. Epigenetics *18*, 2139067.

68. Tatlow, P.J., and Piccolo, S.R. (2016). A cloud-based workflow to quantify transcript-expression levels in public cancer compendia. Sci. Rep. *6*, 39259.

69. Li, B., Senbabaoglu, Y., Peng, W., Yang, M.L., Xu, J., and Li, J.Z. (2012). Genomic estimates of aneuploid content in glioblastoma multiforme and improved classification. Clin. Cancer Res. *18*, 5595–5605.

70. Li, B., Severson, E., Pignon, J.C., Zhao, H., Li, T., Novak, J., Jiang, P., Shen, H., Aster, J.C., Rodig, S., et al. (2016). Comprehensive analyses of tumor immunity: implications for cancer immunotherapy. Genome Biol. *17*, 174.

71. Yoshihara, K., Shahmoradgoli, M., Martínez, E., Vegesna, R., Kim, H., Torres-Garcia, W., Treviño, V., Shen, H., Laird, P.W., Levine, D.A., et al. (2013). Inferring tumour purity and stromal and immune cell admixture from expression data. Nat. Commun. *4*, 2612.

72. Barretina, J., Caponigro, G., Stransky, N., Venkatesan, K., Margolin, A.A., Kim, S., Wilson, C.J., Lehár, J., Kryukov, G.V., Sonkin, D., et al. (2012). The Cancer Cell Line Encyclopedia enables predictive modelling of anticancer drug sensitivity. Nature *483*, 603–607.

73. Maeser, D., Gruener, R.F., and Huang, R.S. (2021). oncoPredict: an R package for predicting in vivo or cancer patient drug response and biomarkers from cell line screening data. Brief. Bioinform. *22*, bbab260.